
Figures and figure supplements

A molecular mechanism of mitotic centrosome assembly in *Drosophila*

Paul T Conduit, et al.

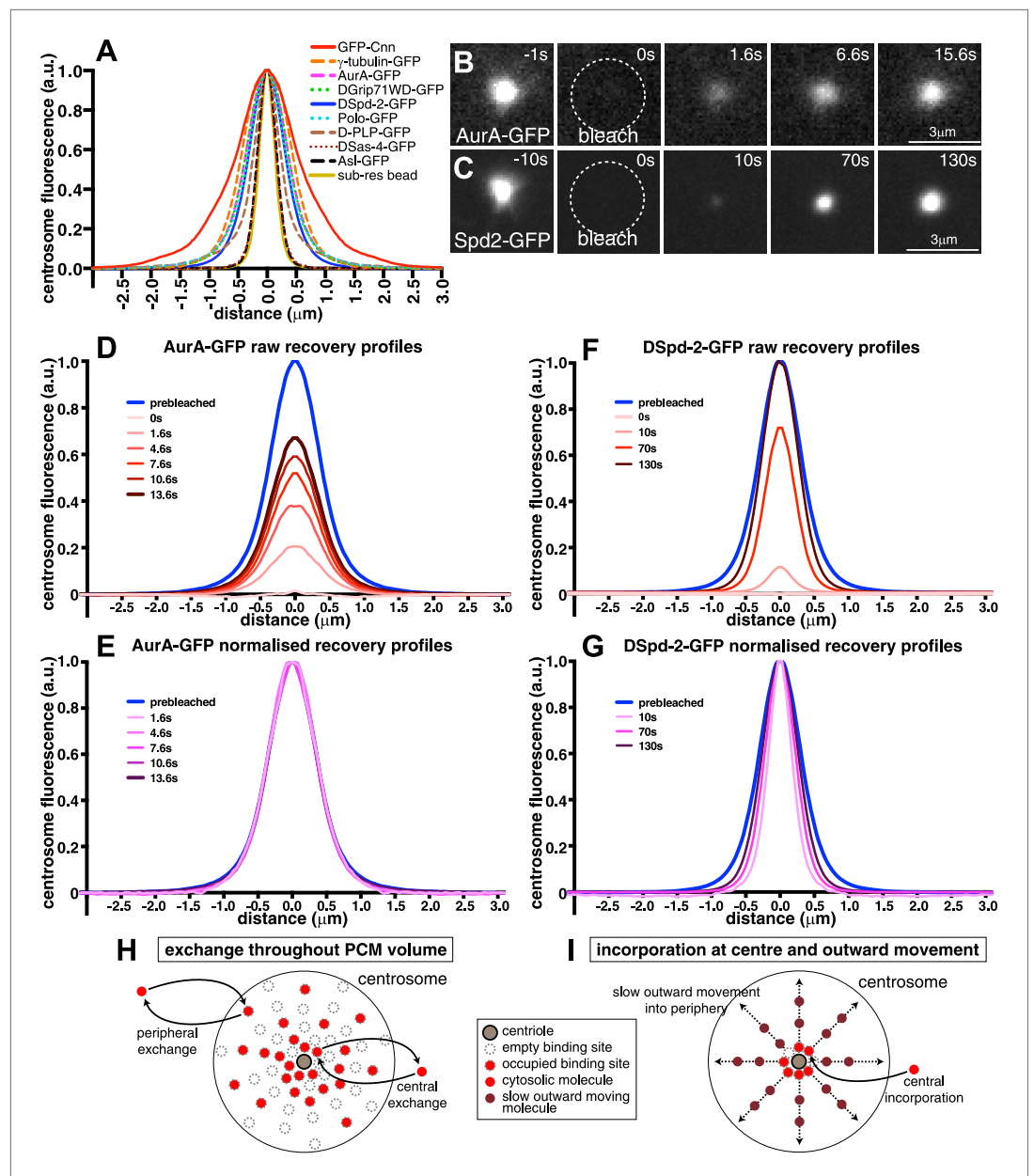


Figure 1. Centrosomal DSpd-2 displays an unusual dynamic behaviour. **(A)** Graph shows the centrosomal fluorescence intensity profiles of various centrosomal proteins, along with the profile of 170 nm sub-resolution beads. **(B)** and **(C)** Images show the FRAP behaviour of AurA-GFP **(B)** and DSpd-2-GFP **(C)**; time before and after photobleaching ($t = 0$) is indicated. Note how AurA-GFP fluorescence appears to recover evenly throughout the region it originally occupied, whereas DSpd-2-GFP fluorescence appears to initially recover only in the centre of the PCM and then spread outward. **(D–G)** Quantification of the recovery dynamics of AurA-GFP **(D)** and **(E)** and DSpd-2-GFP **(F)** and **(G)**. Graphs show the average fluorescence intensity profile of at least 10 centrosomes at the selected time-points after photobleaching: **(D)** and **(F)** show the pre-bleached profiles (blue lines) and successive ‘raw’ recovery profiles (various shades of red), whereas **(E)** and **(G)** show the pre-bleached profiles and successive normalized recovery profiles (various shades of pink/purple—normalized so that their peak intensity is equal to the peak intensity of the pre-bleached profile). The normalized recovery curves of AurA-GFP are essentially identical to the pre-bleached profile at all time-points **(E)**, while for DSpd-2-GFP they are initially narrower and spread outward over time **(G)**. **(H)** and **(I)** Schematics illustrate the dynamic behaviour of AurA-GFP (and most other PCM components) **(H)** and DSpd-2-GFP (and GFP-Cnn) **(I)**. Cytosolic AurA-GFP molecules exchange with binding sites spread throughout the PCM **(H)**, whereas DSpd-2-GFP molecules are recruited by binding sites located close to the

Figure 1. Continued on next page

Figure 1. Continued

centrioles; once released from these binding sites the molecules spread slowly outward into the more peripheral regions of the PCM (I). See also **Figure 1—figure supplements 1 and 2**, and **Video 1**.

DOI: [10.7554/eLife.03399.003](https://doi.org/10.7554/eLife.03399.003)

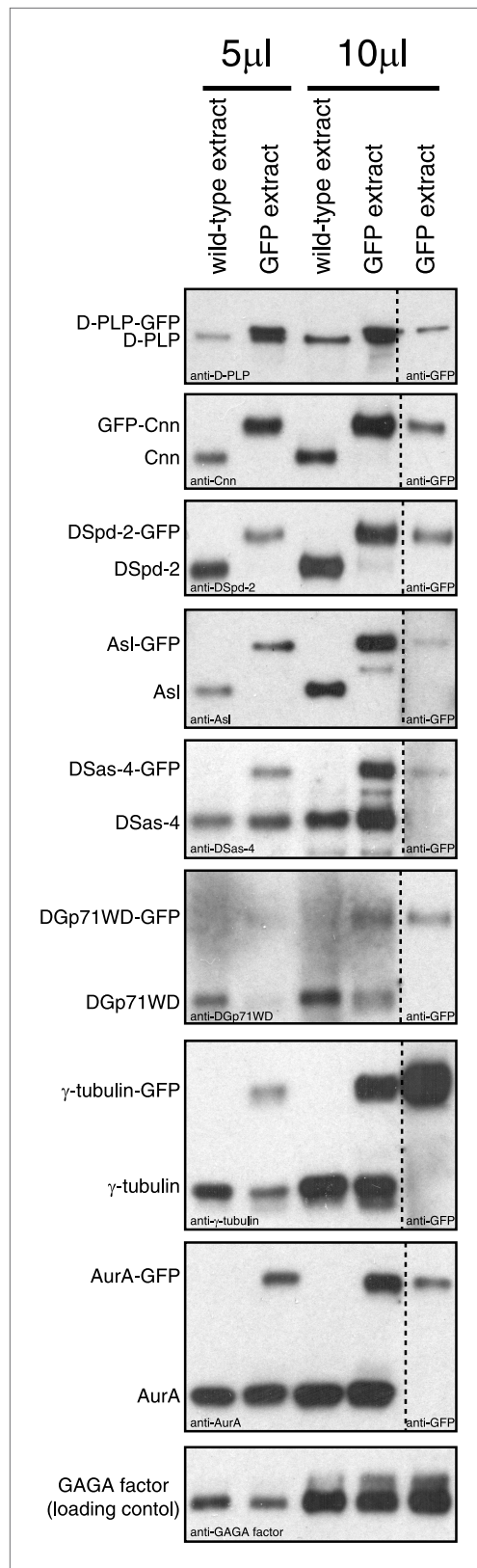


Figure 1—figure supplement 1. An analysis of the expression levels of several GFP-tagged centrosomal proteins. Western blots compare the levels of Figure 1—figure supplement 1. Continued on next page

Figure 1—figure supplement 1. Continued

various centrosomal proteins (as indicated) from wild-type embryo extracts (lanes 1 and 3) or from extracts of embryos expressing a GFP-fused version of the protein (lanes 2, 4, and 5). Lanes 1 to 4 were probed with antibodies raised against the centrosomal protein in question; lane 5 was probed with anti-GFP antibodies. Lanes 1 and 2 were loaded with 5 μ l of extract; lanes 3 to 5 were loaded with 10 μ l of extract. The bottom panel shows a Western blot for GAGA factor, which acts as a loading control (all blots were controlled in this way, but only one example is shown here). GFP-Cnn, DSpd-2-GFP, and Asl-GFP were expressed in a null mutant background; the other GFP-fusions were expressed in a wild-type background. Note how GFP-Cnn and D-PLP-GFP appear to be expressed at slightly higher levels than the endogenous protein, but that the other fusion proteins are expressed either at similar or at slightly lower levels than the endogenous protein. We previously showed that increasing the cytoplasmic concentration of GFP-Cnn increases the rate at which it is incorporated into the PCM, but does not change the inside out incorporation behaviour (**Conduit et al., 2010**). Note also that GFP-Cnn and DSpd-2-GFP are overexpressed and underexpressed, respectively, but both display a similar dynamic behaviour (**Figure 1F,G, Figure 1—figure supplement 2M,N**), again suggesting that the expression level of a GFP-fusion protein does not significantly affect the mode in which it is incorporated into the PCM. We have not been able to analyze the relative expression level of Polo-GFP, as we were unable to get anti-Polo antibodies to work on Western blots.

DOI: [10.7554/eLife.03399.004](https://doi.org/10.7554/eLife.03399.004)

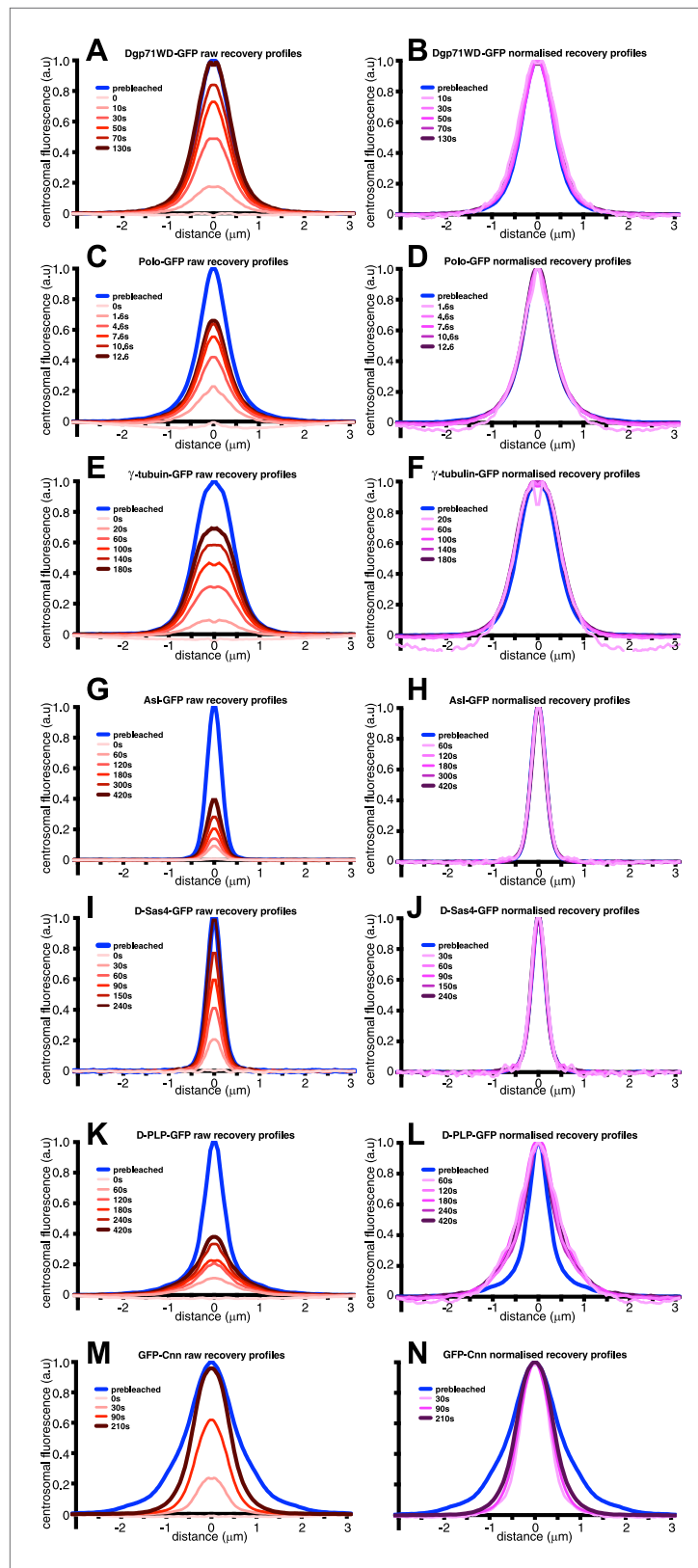


Figure 1—figure supplement 2. An analysis of the dynamic behaviour of several GFP-tagged centrosomal proteins. Quantification of the FRAP recovery dynamics of DGp71WD-GFP (A and B), Polo-GFP (C and D), Figure 1—figure supplement 2. Continued on next page

Figure 1—figure supplement 2. Continued

γ -tubulin-GFP (**E** and **F**), Asl-GFP (**G** and **H**), DSas-4-GFP (**I** and **J**), D-PLP-GFP (**K** and **L**), and GFP-Cnn (**M** and **N**). Graphs show the average fluorescence intensity profile of ≥ 10 centrosomes ('Materials and methods') at selected time-points after photobleaching ($t = 0$). Graphs on the left of each panel display pre-bleached profiles (blue lines) and 'raw' recovery profiles (various shades of red lines). Graphs on the right of each panel display pre-bleached profiles and recovery profiles (various shades of purple lines) that have all been normalized so that their peak intensity is equal to the peak intensity of the pre-bleach profile. Note how the normalized recovery profiles of DGp71WD-GFP (**B**), Polo-GFP (**D**), and γ -tubulin-GFP (**F**) are very similar to their pre-bleached profiles, indicating that they are all incorporated evenly throughout the PCM domain they originally occupied. This is also true for Asl-GFP (**H**) and DSas-4-GFP (**J**), but these proteins have the same distribution as sub-resolution beads (**Figure 1A**), so their true distribution cannot be resolved on this microscope system. The recovery dynamics of D-PLP-GFP (**K** and **L**) are complicated by the presence of a slow-exchanging centriole fraction and a fast-exchanging PCM fraction (**Martinez-Campos et al., 2004**), which cannot be properly distinguished at this resolution. It appears that the slow recovery rate of the centriole fraction compared to the PCM fraction causes the normalized recovery profiles to be wider than the pre-bleached profile. It can be seen, however, that the PCM fraction of D-PLP shows no sign of outward movement through the PCM (**L**). The normalized recovery profiles of GFP-Cnn (**N**) are narrower than the pre-bleached profile and spread outwards over time, reflecting the fact that Cnn molecules are initially incorporated only in the centre of the PCM and then move slowly outward (**Conduit et al., 2014**).

DOI: [10.7554/eLife.03399.005](https://doi.org/10.7554/eLife.03399.005)

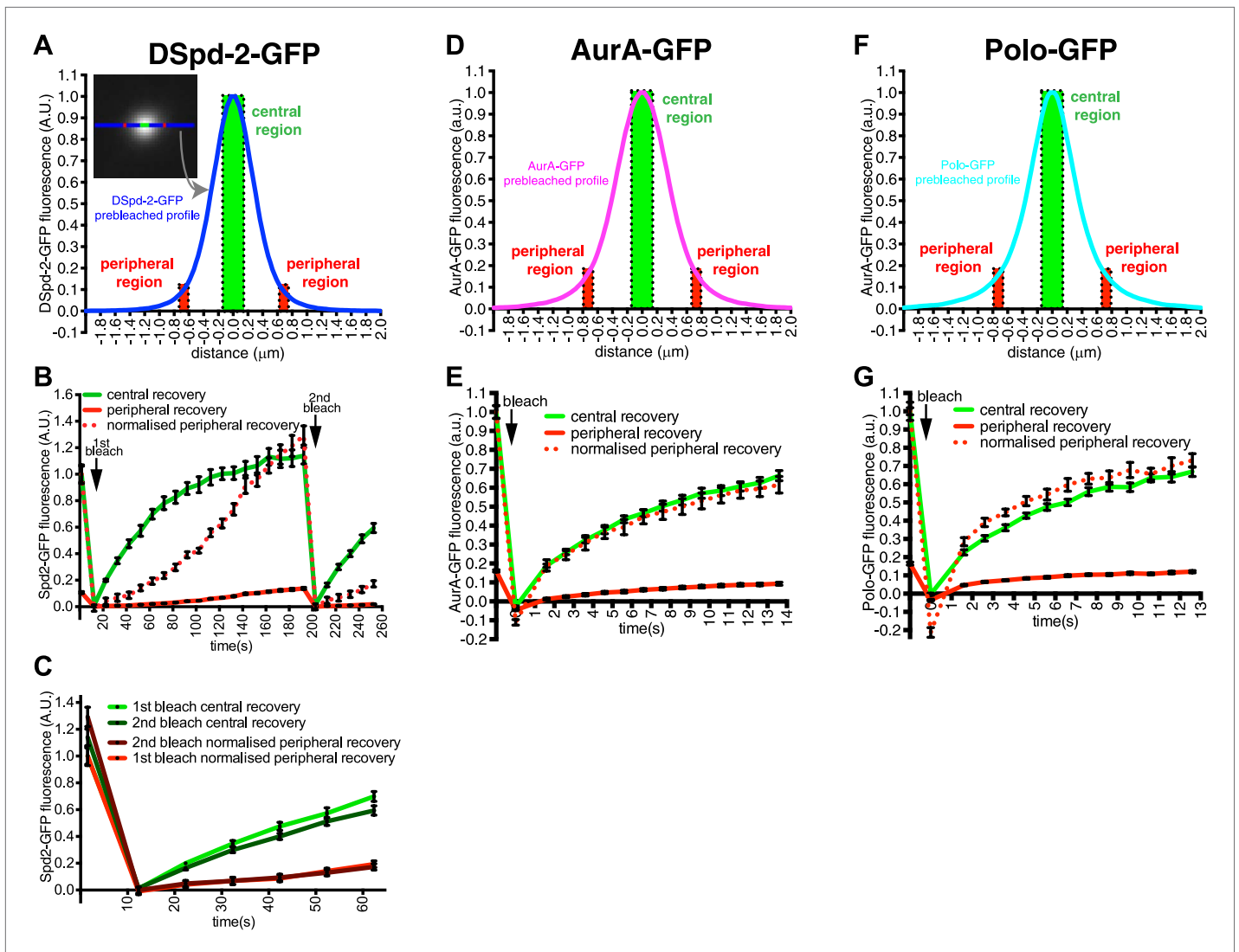


Figure 2. DSpd-2-GFP molecules spread away from the centrioles. **(A)** Graph displays the pre-bleached profile of DSpd-2-GFP at centrosomes in *Drosophila* embryos (blue line, average of 10 centrosomes). Boxes highlight the central region of the PCM (green box) and peripheral regions of the PCM (red boxes) that were analyzed in a FRAP experiment. **(B)** Graph displays the average fluorescence intensity through time in the centre (green line) and periphery (red and dotted red lines) of the PCM after photobleaching. Arrows indicate times of photobleaching. The dotted red line represents the peripheral recovery after it has been normalized so that its initial pre-bleached value is equal to the initial pre-bleached value of the central recovery curve. Note how the central DSpd-2-GFP fluorescence recovery exhibits a typical logarithmic-shaped FRAP curve, with a fast initial rate that slows over time. In contrast, peripheral DSpd-2-GFP fluorescence recovery exhibits a very unusual behaviour as it is initially slow and then speeds up over time. This strongly suggests that DSpd-2-GFP molecules move from the centre to the periphery of the PCM (see main text). **(C)** Graph compares the initial recovery kinetics in the central (green lines) or peripheral (red lines) regions of the PCM after a first (light lines) and then second (dark lines) photobleaching event. The second photobleaching event took place when the rate of recovery in the centre was slow and the rate of recovery in the periphery was fast (see $t = 200$ s in **B**). Note that after the second bleaching event the central recovery returned to its original fast rate and the peripheral recovery returned to its original slow rate, showing that the increasing rate of recovery in the periphery was not due to peripheral binding sites gradually exchanging faster over time. **(D–G)** Graphs display the pre-bleached profiles (**D** and **F**) and recovery kinetics (**E** and **G**) of AurA-GFP (**D** and **E**) and Polo-GFP (**F** and **G**) at centrosomes in embryos (average of 11 centrosomes) in the same format as shown for DSpd-2-GFP (**A** and **B**). Note how the peripheral recovery curves of AurA-GFP (red and dotted red lines in **E**) and Polo-GFP (red and dotted red lines in **G**) both have a similar shape to their central recovery curves, indicating that the unusual peripheral kinetics of DSpd-2-GFP (red and dotted red lines in **B**) are not observed with other proteins that have a similar distribution around the centrioles. Error bars = SEM.

DOI: 10.7554/eLife.03399.007

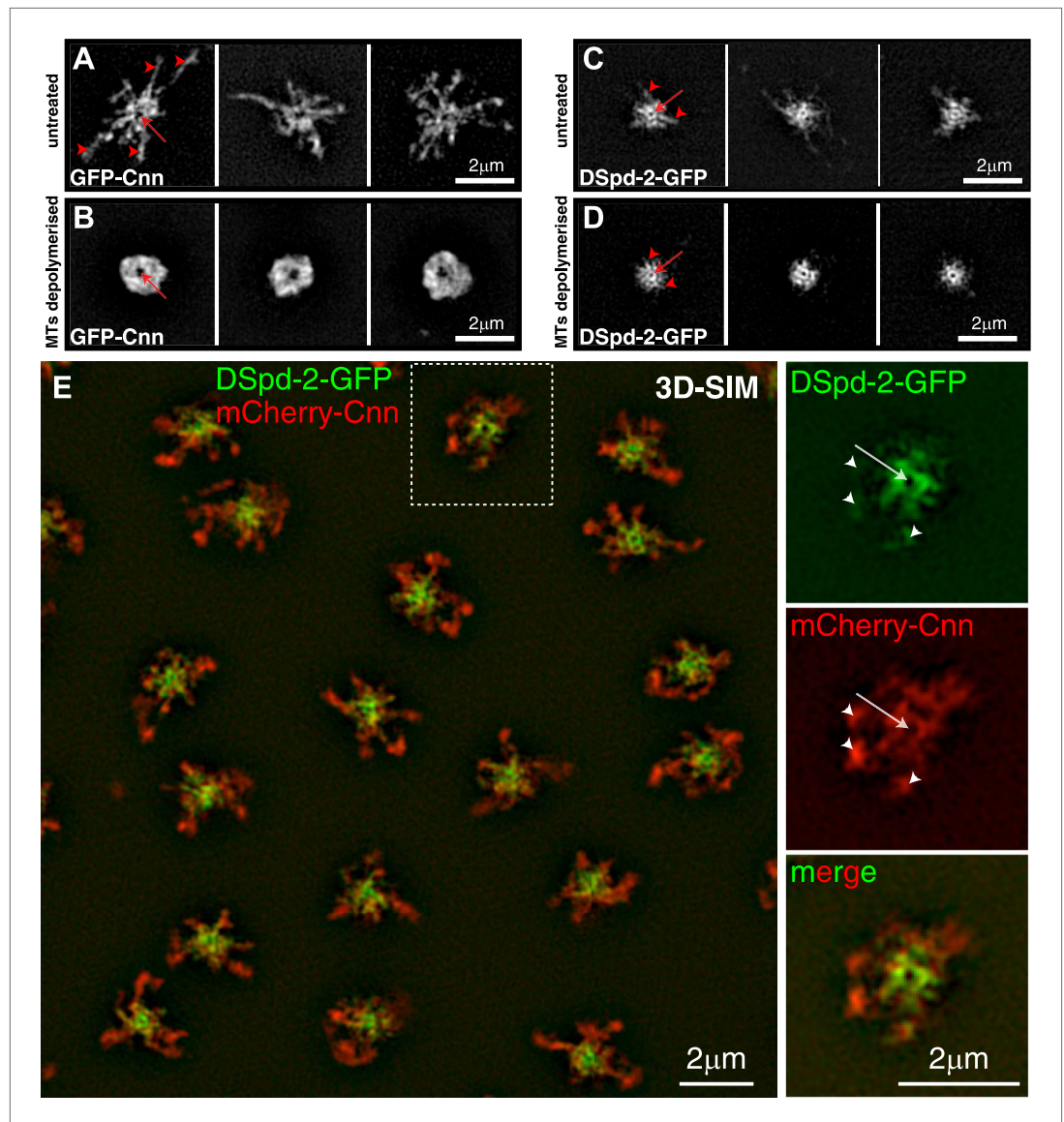


Figure 3. DSpd-2-GFP appears to form scaffold-like structure around the centrosomes that partially co-localizes with the Cnn scaffold. (A–D) 3D-SIM images of centrosomes from embryos expressing either GFP-Cnn (A and B) or DSpd-2-GFP (C and D) where the MTs are either present (A and C) or have been depolymerized by colchicine injection (B and D). (A) In untreated embryos, large projections of GFP-Cnn extend outwards (red arrowheads) from a central hollow (red arrow), which presumably contains the mother centriole. (B) After MT depolymerisation, the GFP-Cnn scaffold collapses into a largely amorphous structure; presumably, the molecular detail of the scaffold cannot be resolved even at this high resolution. The slightly larger central ‘hollow’ in the GFP-Cnn signal (red arrow) likely reflects the ability of the Cnn molecules to move a short distance away from the centre of the centrosome in the absence of microtubules (Conduit *et al.*, 2014); these molecules then get ‘trapped’ in the more peripheral regions of the PCM, as they cannot efficiently leave the centrosome in the absence of MTs (Conduit *et al.*, 2014). (C) In untreated embryos, DSpd-2-GFP appears as a series of spoke-like projections (red arrowheads) that extend away from a central ring (red arrow), which presumably surrounds the mother centriole; some of these projections weakly extend into the peripheral PCM. (D) After MT de-polymerisation, DSpd-2-GFP retains a large degree of its structure: there is a clear central ring (red arrow) with several spoke-like projections extending outwards (red arrowheads); these projections, however, no longer appear to extend into the more peripheral regions of the PCM. (E) Two-colour 3D-SIM images of centrosomes in untreated embryos co-expressing DSpd-2-GFP (green) and mCherry-Cnn (red). The panels on the right are enlargements of the boxed centrosome in the panel on the left; note the clear hollow in the centre of the centrosome (arrows), and how the mCherry-Cnn signal extends further

Figure 3. Continued on next page

Figure 3. Continued

away from the centrioles than the DSpd-2-GFP signal, although weak DSpd-2-GFP fluorescence can often be observed in the same region as the more peripheral mCherry-Cnn (arrowheads). See also **Figure 3—figure supplement 1**.

DOI: [10.7554/eLife.03399.008](https://doi.org/10.7554/eLife.03399.008)

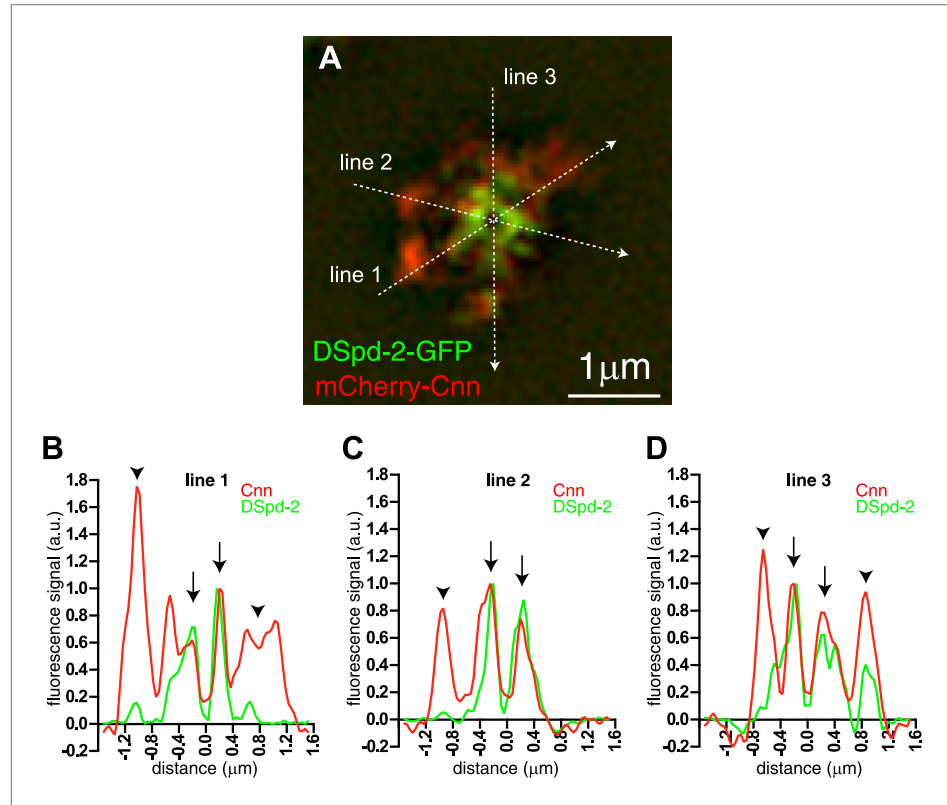


Figure 3—figure supplement 1. An approximate quantification of mCherry-Cnn and DSpd-2-GFP co-localisation. The mCherry-Cnn (red) and DSpd-2-GFP (green) fluorescence intensity along the three lines that run through a 3D-SIM image of a centrosome in (A) are plotted on the graphs in (B), (C), and (D). Green lines represent the fluorescent intensity of DSpd-2-GFP, and red lines represent the fluorescent intensity of mCherry-Cnn. The graphs have been normalized so that the peak value in the central region of the PCM is equal to 1. Arrows within the graphs indicate the central regions of the centrosome where mCherry-Cnn and DSpd-2-GFP extensively co-localize. Arrowheads indicate the more peripheral regions of the centrosome that contain high levels of mCherry-Cnn fluorescence but only low levels of DSpd-2-GFP fluorescence.

DOI: [10.7554/eLife.03399.009](https://doi.org/10.7554/eLife.03399.009)

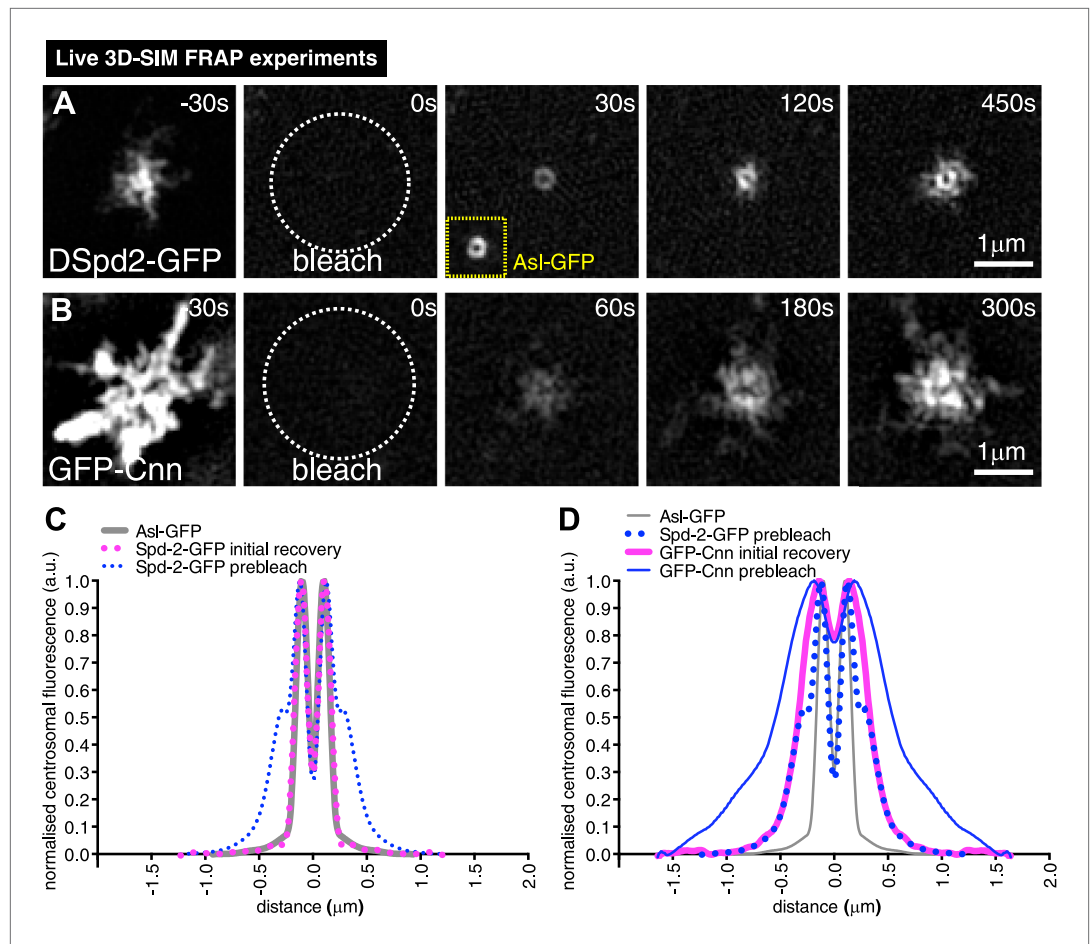


Figure 4. 3D-SIM FRAP analysis of DSpd-2-GFP and GFP-Cnn behaviour at centrosomes. **(A and B)** 3D-SIM images show the dynamic behaviour of DSpd-2-GFP **(A)** and GFP-Cnn **(B)** at centrosomes in living *Drosophila* embryos after FRAP; time before and after photobleaching ($t = 0$) is indicated. **(A)** DSpd-2-GFP fluorescence initially recovers in a toroid shape around the centriole **(A, $t = 30$ s)**, which has similar dimensions to unbleached AsI-GFP (yellow inset). The protein then moves slowly outwards, forming dynamic projections that spread away from the centriole. **(B)** GFP-Cnn fluorescence initially recovers in a broader region around the centrioles ($t = 60$ s in **B**), which has similar dimensions to the pre-bleached DSpd-2-GFP signal ($t = -30$ s in **A**). **(C)** Graph compares the average prebleached (dotted blue line) and initial recovery (dotted pink line) profiles of DSpd-2-GFP to the average unbleached profile of AsI-GFP (grey line); all profiles were normalized so that their peak value is equal to 1. Note how the initial DSpd-2-GFP recovery profile is essentially identical to the un-bleached AsI-GFP profile. **(D)** Graph compares the average pre-bleached (solid blue line) and initial recovery (solid pink line) profiles of GFP-Cnn, to the average pre-bleached profile of DSpd-2-GFP (dotted blue line), and the average unbleached profile of AsI-GFP (grey line); all profiles were normalized so that their peak value is equal to 1. Note how the initial GFP-Cnn recovery profile is very similar (particularly in the more peripheral regions), to the pre-bleached DSpd-2-GFP profile, but is quite distinct from the pre-bleached AsI-GFP profile. See also **Video 2**.
DOI: 10.7554/eLife.03399.010

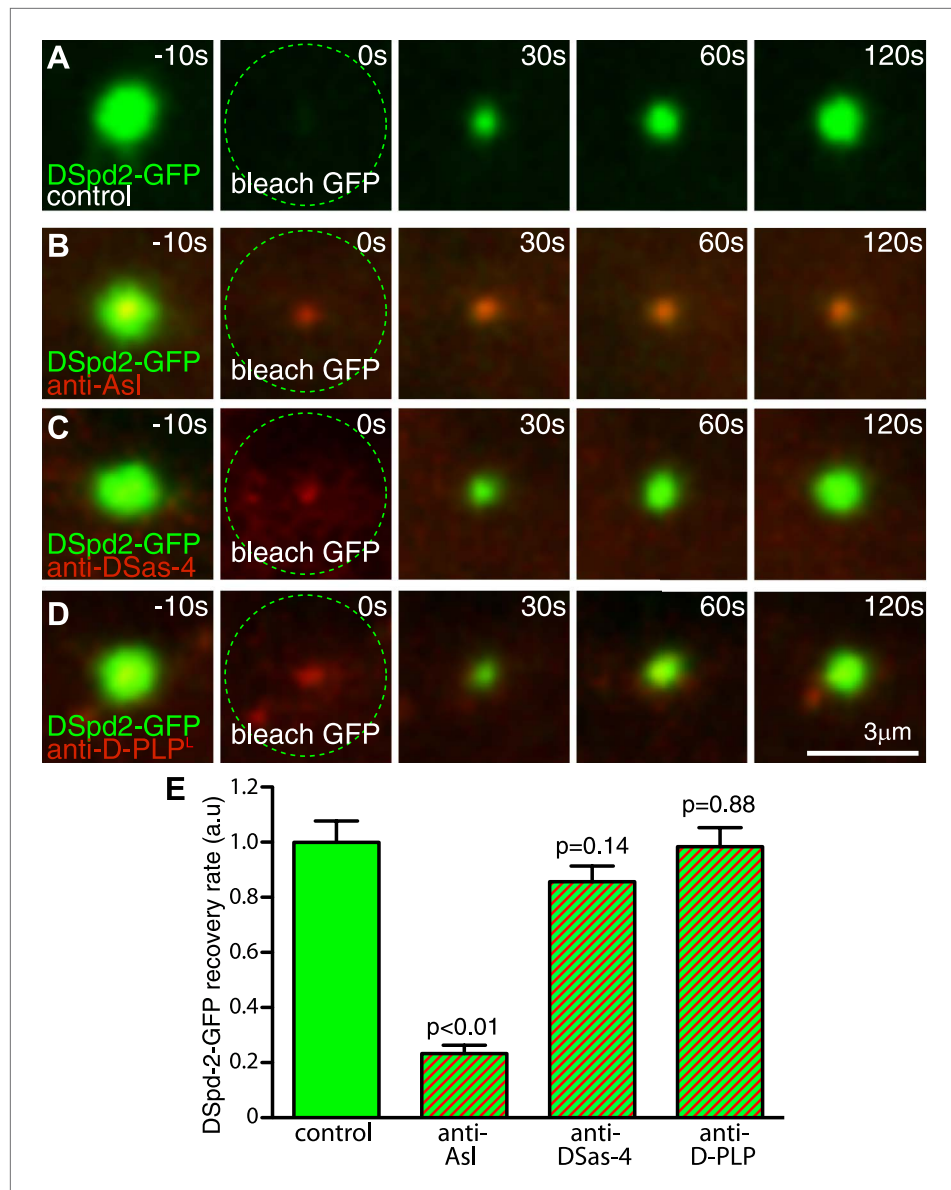


Figure 5. Inhibiting Asl function strongly perturbs DSpd-2 incorporation into the PCM. Images (A–D) show results from FRAP experiments monitoring how DSpd-2-GFP (green) incorporation into the PCM is affected by inhibiting the function of various centriole-associated components with injected Texas-red-labelled antibodies (red—as indicated). The antibodies bind to their cognate protein at centrosomes close to the injection site (B–D), but not to those far from the injection site (A), which therefore act as internal controls. (E) Graph displaying the initial recovery rate of DSpd-2-GFP fluorescence at centrosomes bound with antibodies (as indicated below the graph) relative to the centrosomes not bound by antibodies (control). The rate of recovery was calculated by measuring the gradient of the initial linear phase of recovery that occurred over the first 60 s after photobleaching. Note how anti-Asl antibodies reduce the rate of DSpd-2-GFP incorporation into the PCM by ~75%, but that anti-DSas-4 or anti-D-PLP antibodies have little or no effect. Error bars = standard error. See also **Video 3**. DOI: [10.7554/eLife.03399.012](https://doi.org/10.7554/eLife.03399.012)

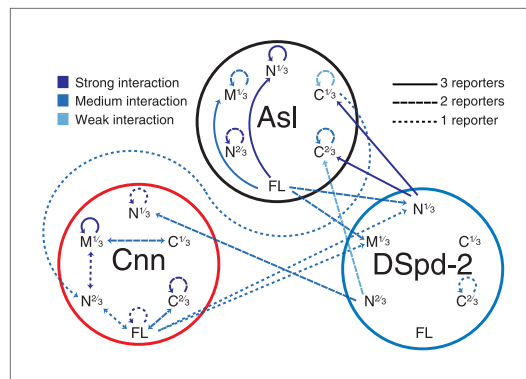


Figure 6. A yeast-two-hybrid analysis examining the interactions between Asl, DSpd-2, and Cnn. A schematic summary of the yeast two-hybrid interactions observed between Asl, DSpd-2, and Cnn. The shades of the lines indicate the strength of the interactions observed: strong (dark blue), medium (blue), and weak (light blue). The characteristics of the lines indicate the number of different positive reporter assays for each interaction: solid line (3/3 assays), large dashed line (2/3 assays), and small dashed line (1/3 assays). Arrows point from bait to prey fragments—double-headed arrows indicate that the interaction scored positive with either fragment as bait or prey. See **Figure 6—source data 1**. DOI: [10.7554/eLife.03399.014](https://doi.org/10.7554/eLife.03399.014)

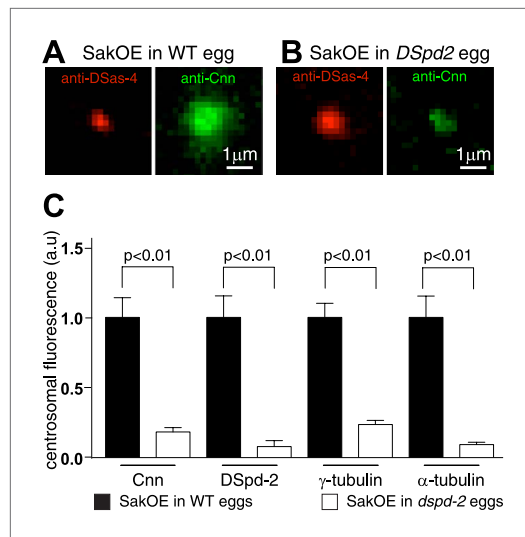


Figure 7. The centrosomal levels of Cnn are strongly reduced in eggs lacking DSpd-2. **(A and B)** Images show centrosomes co-stained with DSas-4 antibodies (red) and Cnn antibodies (green) in fixed eggs that either contained **(A)** or lacked **(B)** endogenous DSpd-2. As embryos lacking DSpd-2 fail in pronuclear fusion (**Dix and Raff, 2007**) (and so fail to develop), we induced the de novo formation of centrosomes in WT and DSpd-2 mutant eggs by over-expressing Sak kinase (**Peel et al., 2007; Rodrigues-Martins et al., 2007**). The centrosomal levels of Cnn are dramatically reduced in the absence of DSpd-2. **(C)** The graph quantifying the centrosomal levels of Cnn, DSpd-2, γ -tubulin, and α -tubulin in Sak over-expressing eggs that either contained (black bars) or lacked (white bars) endogenous DSpd-2. The centrosomal levels of Cnn, γ -tubulin, and α -tubulin are dramatically reduced in the absence of DSpd-2.

DOI: [10.7554/eLife.03399.016](https://doi.org/10.7554/eLife.03399.016)

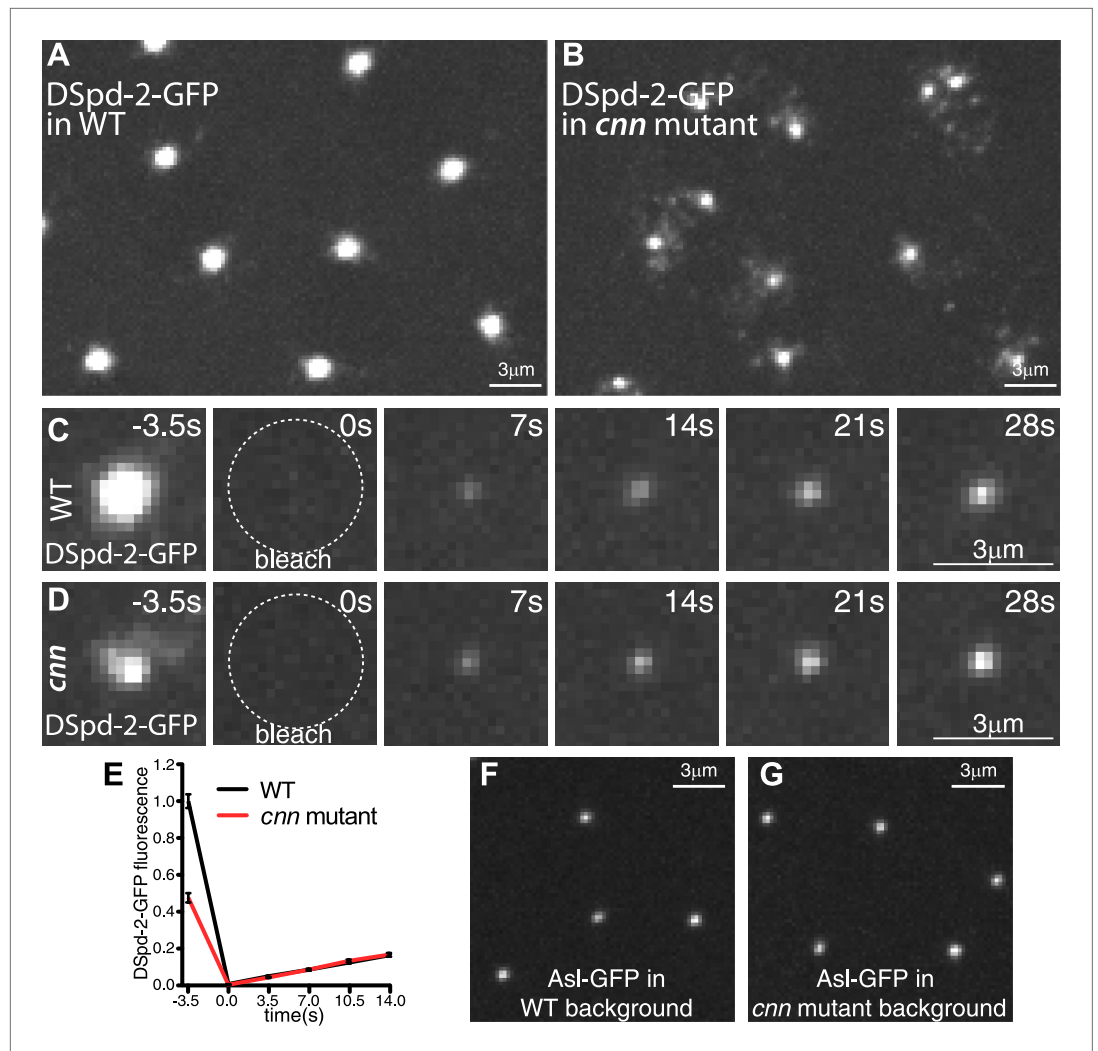


Figure 8. Cnn helps maintain DSpd-2 in the PCM. **(A and B)** Images show the localization of DSpd-2-GFP at centrosomes in either WT **(A)** or *cnn* mutant **(B)** embryos. **(C and D)** Images show the initial dynamic behaviour of DSpd-2-GFP at centrosomes in either WT **(C)** or *cnn* mutant **(D)** embryos; time before and after photobleaching ($t = 0$ s) is indicated. **(E)** Quantification of DSpd-2-GFP fluorescence recovery at centrosomes in either WT (black line) or *cnn* mutant (red line) embryos. The initial rate of DSpd-2-GFP fluorescence recovery is very similar in both WT and *cnn* mutant embryos, revealing that the initial incorporation of DSpd-2-GFP into the PCM is not dependent on Cnn. **(F and G)** Images show the localization of Asl-GFP at centrosomes in living embryos in the presence **(F)** or absence **(G)** of Cnn. The ability of Asl to localize efficiently in the absence of Cnn presumably explains why DSpd-2 can still be recruited to centrioles at normal rates in the absence of Cnn. Error bars = standard error. See **Video 4**. DOI: 10.7554/eLife.03399.017

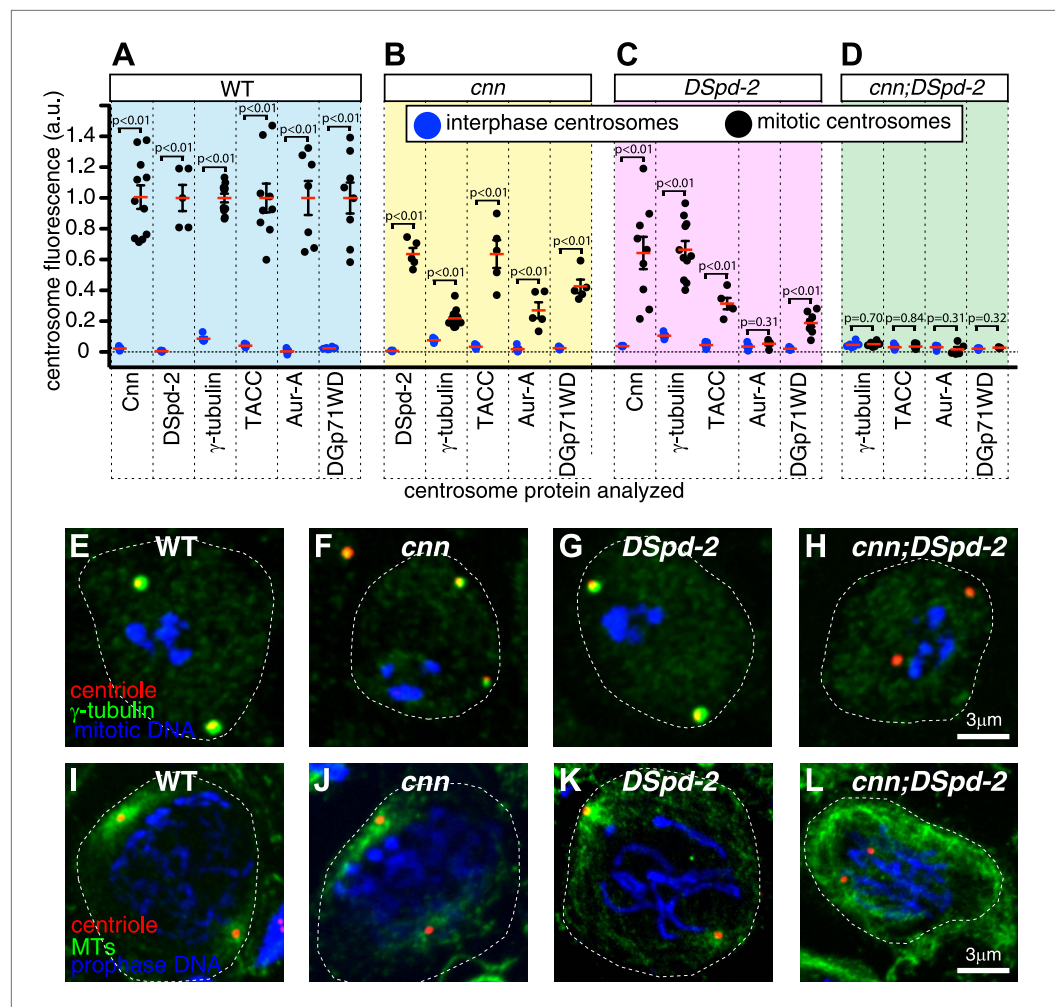


Figure 9. Cnn and DSpd-2 cooperate to recruit the mitotic PCM. (A–D) Graphs show the average fluorescence intensities of interphase (blue dots) and mitotic (black dots) centrosomes from either WT (A), *cnn* mutant (B), *dspd-2* mutant (C), or *cnn;dspd-2* double mutant (D) larval brain cells stained for various centrosomal proteins (as indicated below graphs). Each data-point represents the average centrosome value from one brain. The horizontal red bars indicate the average value of all the brains. All the PCM proteins are still partially recruited to centrosomes in the absence of Cnn or DSpd-2 (with the possible exception of Aurora A, which does not appear to be recruited in the absence of DSpd-2). The mitotic PCM levels do not rise above interphase levels in the absence of both Cnn and DSpd-2, indicating that centrosome maturation has been abolished. (E–L) Images show typical mitotic cells from either WT (E and I), *cnn* (F and J), *dspd-2* (G and K), or *cnn;dspd-2* double mutant (H and L) larval brain cells stained for the centriole marker Asl (red), mitotic DNA (phospho-histone H3, blue), and either the PCM marker γ -tubulin (green, E–H) or MTs (I–L, green). Error bars = SEM. See also **Figure 9—figure supplements 1 and 2**. DOI: 10.7554/eLife.03399.019

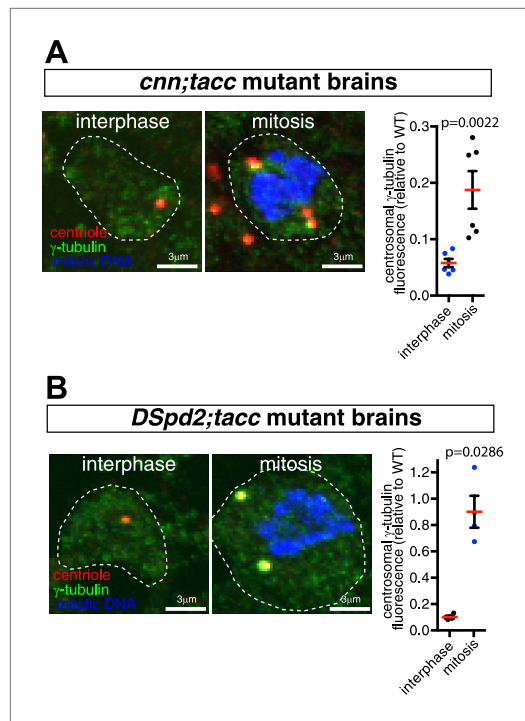


Figure 9—figure supplement 1. Centriosome maturation is not abolished in *cnn;tacc* or *dspd-2;tacc* double mutants. **(A and B)** Images and associated graphs show mitotic and interphase larval brain cells stained for γ -tubulin (green), the centriole marker Asl (red), and mitotic DNA (phospho-histone H3, blue) from either *cnn;tacc* double mutant **(A)** or *dspd-2;tacc* double mutant larvae **(B)**. Graphs display the average fluorescent intensities of mitotic and interphase centrosomes (relative to a WT mitotic value of 1) stained for γ -tubulin. Each data-point represents the average centrosome value from one brain. Note how centrosomes still partially mature in each mutant combination, as the levels of γ -tubulin centrosomal fluorescence are significantly higher in mitotic cells than in interphase cells.

DOI: [10.7554/eLife.03399.020](https://doi.org/10.7554/eLife.03399.020)

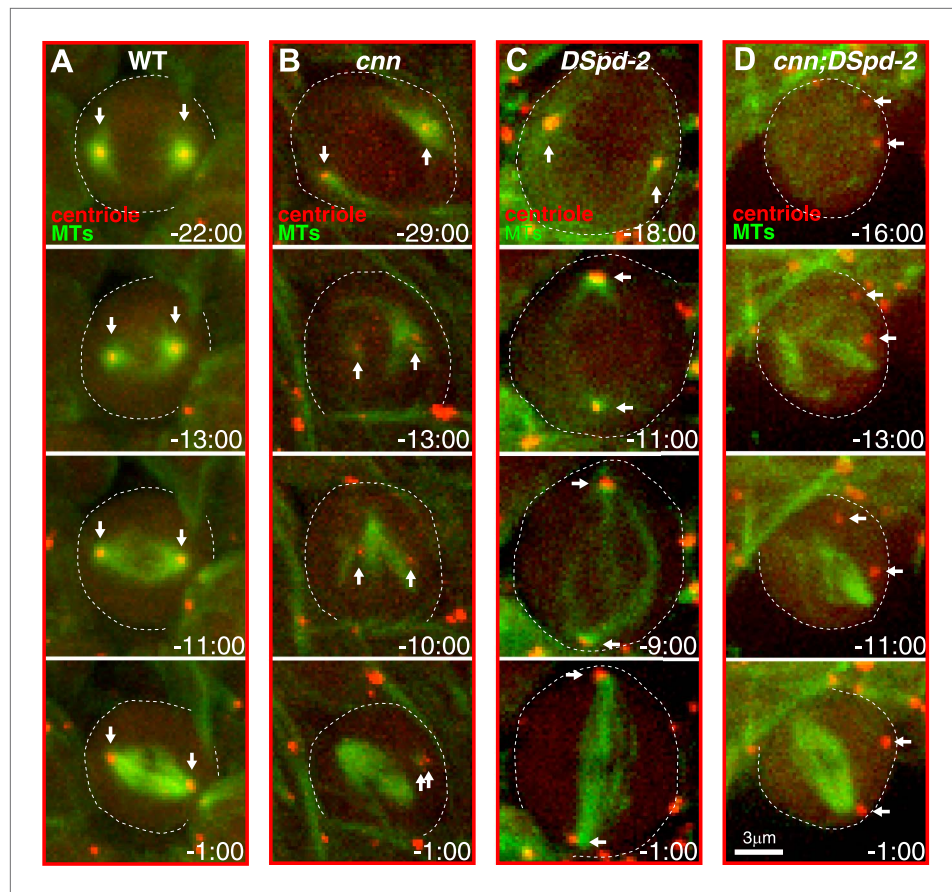


Figure 9—figure supplement 2. Centrosomes in *cnn;dspd-2* double mutants fail to organize MTs. Images show selected time-points from videos of either WT (A), *cnn* (B), *dspd-2* (C), or *cnn;dspd-2* double mutant (D) brain cells expressing the MT marker Jupiter-mCherry (pseudo-coloured green) and the centriole marker GFP-PACT (pseudo-coloured red); time before and after anaphase onset ($t = 0$ s) is indicated. Arrows indicate the position of the centrosomes. The centrosomes in WT cells, or *cnn* or *dspd-2* single mutant cells can organize MT asters, but no centrosome-associated MTs can be detected in the *cnn;dspd-2* double mutants.

DOI: [10.7554/eLife.03399.021](https://doi.org/10.7554/eLife.03399.021)

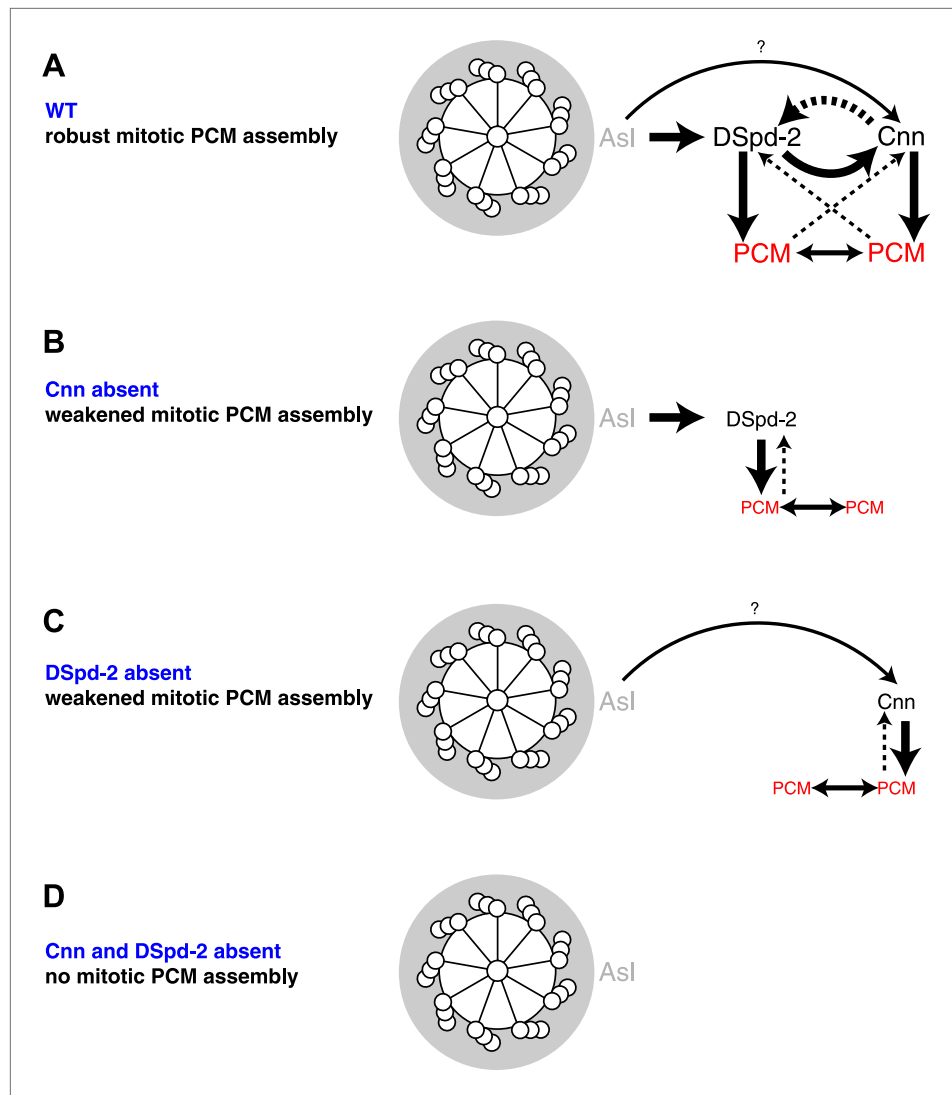


Figure 10. A model for mitotic PCM assembly in flies. Schematics illustrate a putative pathway of mitotic PCM assembly in a WT cell (**A**), or in cells lacking either Cnn (**B**), DSpd-2 (**C**), or both Cnn and DSpd-2 (**D**). A top view of the mother centriole is shown surrounded by a layer of Asl (grey); solid arrows represent recruiting interactions, dotted arrows represent maintaining interactions. Arrow thickness reflects the relative strength of the recruitment or maintenance, and the size of the text reflects the amount of protein localized at centrosomes. In WT cells (**A**), Asl has an important role in recruiting DSpd-2 to centrosomes, which in turn has an important role in recruiting Cnn; Cnn then has an important role in maintaining DSpd-2 at centrosomes. Thus, a positive feedback loop is generated where increasing amounts of DSpd-2 can recruit increasing amounts of Cnn, which can then maintain increasing amounts of DSpd-2. DSpd-2 and Cnn both independently recruit other PCM components (red), which themselves help support the PCM structure and can recruit further PCM components. In the absence of Cnn (**B**), Asl can still recruit DSpd-2 normally, but DSpd-2 cannot efficiently accumulate around the centrioles. The reduced levels of DSpd-2 recruit reduced levels of PCM. In the absence of DSpd-2 (**C**), an alternative pathway recruits reduced levels of Cnn. This pathway most likely involves Asl (as indicated here), as inhibiting Asl reduces the rate of Cnn incorporation into the PCM (Conduit et al., 2010) and Asl and Cnn appear to weakly interact in a Y2H analysis (Figure 6); other pathways, however, could also be involved. The reduced levels of Cnn recruit reduced levels of PCM. In the absence of Cnn and DSpd-2 (**D**), no mitotic PCM can be assembled.

DOI: [10.7554/eLife.03399.023](https://doi.org/10.7554/eLife.03399.023)